Adaptive Error-Correction Coding Scheme for Underwater Acoustic Communication Networks

Roee Diamant and Lutz Lampe
University of British Columbia, Vancouver, BC, Canada, Email: {roeed,lampe}@ece.ubc.ca

***Abstract*—Underwater acoustic communication networks (UWANs) have recently attracted much attention in the research community. Two properties that set UWANs apart from most radio-frequency wireless communication networks are the long propagation delay and the possible sparsity of the network topology. This in turn offers opportunities to optimize throughput through time and spatial reuse. In this paper, we propose a new adaptive coding method to realize the former. We consider time-slotted scheduling protocols, which are a popular solution for contention-free and interference-free access in small-scale UWANs, and exploit the surplus guard time that occurs for individual links for improving transmission reliability. In particular, using link distances as side information, transmitters utilize the available portion of the time slot to adapt their code rate and increase reliability. Since increased reliability trades off with energy consumption for transmission, we optimize the code rate for best trade-off, considering both single and multiple packet transmission using the incremental redundancy hybrid automatic repeat request (IR-HARQ) protocol. For practical implementation of this adaptive coding scheme we consider punctured and rateless codes. Simulation results demonstrate the gains achieved by our coding scheme over fixed-rate error-correction codes in terms of both throughput and consumption of transmitted energy per successfully delivered packet. We also report results from a sea trial conducted at the Haifa harbor, which corroborate the simulations.**

***Index Terms*—Underwater acoustic communication, Adaptive coding, Rate-less codes, Incremental redundancy automatic repeat request (IR-HARQ)**

, where the number of network nodes is relatively small, transmission distance is large, and frequent packet exchange allows distance estimation.

I. Introduction

Reliable underwater acoustic communication is challenging due to the limited available transmit power and bandwidth, large channel attenuation and long channel delay, as well as time-varying channel conditions with large Doppler spread [1]. In this paper, we focus on improving reliability for time-slotted underwater acoustic communication networks (UWANs). Slotted scheduling is especially attractive in UWANs, where networks are often small and, due to low transmission rates, possible clock drifts are negligible compared to the packet length [2]. We consider a set of applications where packets are frequently exchanged, which allows distance estimation. These include sharing of navigation information, control of autonomous underwater vehicles (AUV), and undersea command and control. A practical example we have in mind is a system called ”Deep-Link”, which is used for command and control, surveillance, and diver-safety purposes in three navies. Nodes in the Deep-Link system operate in a spatial-reuse time-division-multiple-access (TDMA) network and periodically broadcast packets with location information to nodes up to 5 km away (see system specification in [3]).

Due to the usually low reliability of communication in UWANs, the use of adaptive coding schemes has been considered in literature. Adaptive coding can be done by transmitter-side adjustment of code rate or by receiver-initiated request of additional transmissions, i.e., automatic repeat request (ARQ), to ensure successful data delivery. With regards to the latter, incremental redundancy hybrid ARQ (IR-HARQ) is particularly efficient as it does not suffer from a coding loss due to repetition of the same parity symbols [4]. Despite the coding efficiency of IR-HARQ, it suffers from high latency due to retransmission requests and retransmissions. Due to the long propagation delay of sound transmission and the low link reliability, this disadvantage is particularly pronounced in UWANs. In part addressing this problem, several adaptive transmission applications tailored to UWANs have been suggested. In [5], an adaptive modulation scheme was implemented to optimize transmission rate for time-varying channel conditions. In [6], an HARQ using rateless codes has been suggested for transferring large files underwater. A rateless coding scheme is also used in [7] to optimize throughput of UWANs for broadcast communications. Another ARQ method has been developed in [8], where retransmissions are opportunistically scheduled to improve network reliability. Finally, relying on feedback from the intended receiver, an adaptive coding scheme was recently offered in [9], where the transmitter and receiver collaborate to optimize the code rate for the current channel conditions.

While the existing literature demonstrated significant improvement in network throughput and latency, we argue that there is room for further improvement by obtaining channel state information (CSI) in the form of *distance* to nearby nodes. Since in slotted scheduling, the guard interval is usually dimensioned according to the modem’s maximal detection range (which for UWANs corresponds to a propagation delay on the order of a few seconds for a typical interference range of a few kilometers [1]), each (re)transmission includes a sizeable overhead. Thus, considering that actual propagation delay for specific communication links is often notably shorter than the maximal expected delay, in this paper we suggest improving link reliability by utilizing the often over-sized guard interval in a time slot. In particular, assuming that the propagation delays to nodes within the interference range of a transmitting node are known (e.g., from frequent packet exchange, such as from navigation packets in Deep-Link), our

scheme opportunistically includes extra parity symbols in the data packet if the guard interval is longer than needed for interference-free transmission. Since extending the code length trades off reliability and energy consumption for transmission, we optimize the number of parity symbols used, considering both single packet transmission and packet retransmission with IR-HARQ. We note that compared to conventional adaptive coding, where CSI usually is given in the form of a link quality parameter like signal-to-noise ratio (SNR), one novel aspect of our approach lies in the use of ranging information as part of the CSI. Furthermore, while several approaches have been suggested to utilize the long propagation delay in the channel by transmitting more data in the channel (e.g., [8], [10], [11]), the adaptation of coding rate based on delay has not been considered before.

We present two possible implementations for our adaptive coding approach, one based on a bank of codes and another one based on rateless codes. For both schemes, we include the case of ranging information being available only at the transmitter side, thus obtaining range-based adaptive coding with no communication overhead. We present simulation results for typical underwater acoustic environments as well as experimental results from a sea trial. The results demonstrate that, when ranging information is available (e.g., the Deep-Link application), our protocol provides significant gains compared to the performance of fixed coding schemes in both reliability and transmission energy consumption.

The remainder of this paper is organized as follows. The details of the system model are introduced in Section II. In Section III, we describe our adaptive coding approach for both single packet transmission and IR-HARQ. Two possible implementations schemes of the proposed adaptive coding method are introduced in Section IV. Simulation and experimental results are presented and discussed in Section V, and conclusions are drawn in Section VI.

II. System Model

We consider slotted UWANs where node i is assigned with messages of K information symbols to transmit to its designated receiver j. The considered scenario accommodates unicast communication, and besides slotted transmissions, we set no limitation on the scheduling protocol. We define the link interference range as the distance up to which transmissions significantly affect the signal-to-interference-plus-noise ratio (SINR) at an unintended receiver. Due to the large attenuation in the underwater acoustic channel (cf. [1]) we assume that the per-link interference range can be bounded by the detection range of synchronization signals, whose energy is usually much larger than that of information bearing signals. We assume periodic packet exchange between nodes, such that by estimating the time-of-flight [12], [13] of received synchronization signals, each node is aware of the distance to nodes located within its interference range.

Let $d^{\max}$ be the maximal interference range of the system. Furthermore, for time slot t, let $d_{t,i}$ be the maximum distance of node i to nodes within its interference range which are scheduled to receive in time-slots t and $t+1$. Clearly,

$$d_{t,i} \leq d^{\max} \,, \tag{1}$$

and thus often the guard interval could be reduced while still ensuring that packets are received interference-free. Using knowledge of $d_{t,i}$, our goal is to optimize time slot utilization of node i. The optimization aims to strike a balance between reliability of and energy consumption for transmission.

III. The Adaptive Coding Scheme

Let us first consider the transmission of a single packet, i.e., no ARQ is applied. If a fixed-rate error-correction code is used, K information symbols are encoded into $N^{\min}$ coded symbols. $N^{\min}$ is determined assuming $d_{t,i} = d^{\max}$ and thus the full guard interval is needed for interference-free scheduling. However, assuming that node i has an accurate estimate of the range difference

$$\Delta_{t,i} = d^{\max} - d_{t,i} \,, \tag{2}$$

we can shorten the guard interval and transmit up to

$$N_{t,i}^{\max} = \lfloor N^{\min} + \frac{\Delta_{t,i}}{T_{\mathrm{s}} \cdot c} \rfloor \tag{3}$$

symbols without causing interference to other unintended receivers. In (3), T_{s} and c are the symbol period and propagation speed, respectively. Hence, denoting by $N_{t,i}^{\mathrm{actual}}$ the number of actually transmitted symbols transmitted at time t from source i, then $N^{\min} \leq N_{t,i}^{\mathrm{actual}} \leq N_{t,i}^{\max}$.

Next, we demonstrate the gain that can be achieved by adaptive coding in terms of the packet-error-rate (PER) and the energy consumption for transmission. This not only highlights the possible improvements by better utilizing the time slot, but also sets the stage for the following optimization of $N_{t,i}^{\mathrm{actual}}$.

A. Gain of Adaptive Coding

We use the example of an (K, N) Reed-Solomon (RS) code [14] to analyze the performance improvements due to adaptive coding.

1) PER Gain: Let N' be the number of transmitted symbols after puncturing $N - N'$ symbols of the original RS code. Denoting by p^{RS} the RS symbol error probability before decoding, the packet error probability (PER) after decoding is given by

$$p_{\mathrm{packet}}^{\mathrm{RS}}(N') = \sum_{k=\lfloor (N'-K)/2 \rfloor + 1}^{N'} \binom{N'}{k} (p^{\mathrm{RS}})^k (1-p^{\mathrm{RS}})^{N'-k} \,. \tag{4}$$

Let us consider the PER when the receiver obtains $N' = N_{t,i}^{\mathrm{actual}}$ demodulated symbols, and compare it to the case of coding with $N^{\min}$. By (4), the PER of these schemes is $p_{\mathrm{packet}}^{\mathrm{RS}}(N_{t,i}^{\mathrm{actual}})$ and $p_{\mathrm{packet}}^{\mathrm{RS}}(N^{\min})$, respectively. Thus, in terms of success rate, the gain of the adaptive punctured RS coding scheme over the fixed code is

$$g_{\mathrm{coding}} = \frac{1 - p_{\mathrm{packet}}^{\mathrm{RS}}(N_{t,i}^{\mathrm{actual}})}{1 - p_{\mathrm{packet}}^{\mathrm{RS}}(N^{\min})} \,. \tag{5}$$

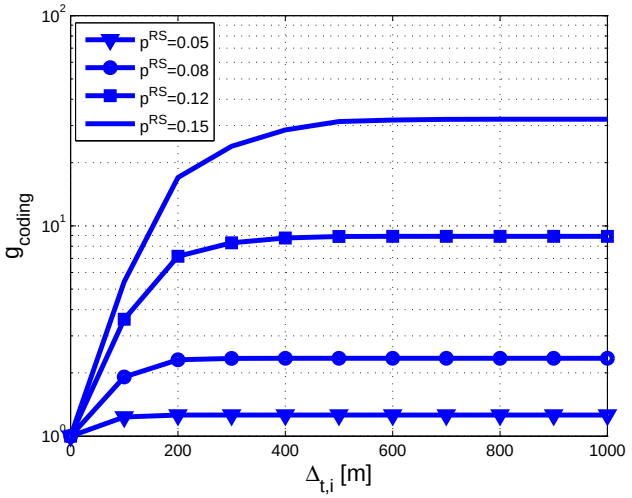

Fig. 1: Gain g_{coding} from (5) as a function of $\Delta_{t,i}$ from (2).

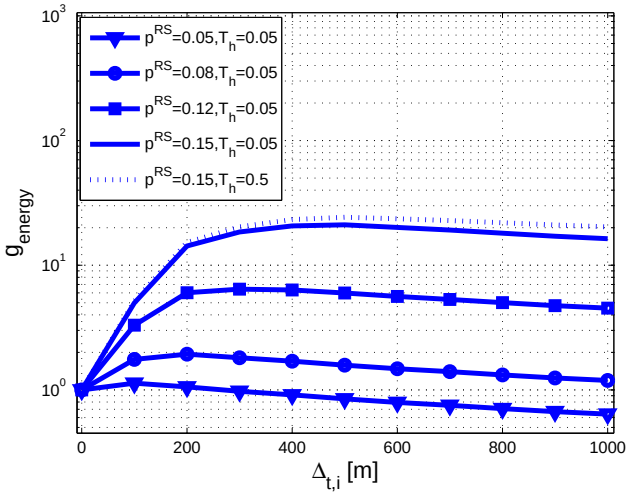

Fig. 2: Gain g_{energy} from (7) as a function of T_{h} and $\Delta_{t,i}$ from (2). Non-erasure channel.

In Figure 1, for $T_{\text{s}} = 0.01$ sec, $c = 1500$ m/sec, we show g_{coding} from (5) for $N_{t,i}^{\text{actual}} = N_{t,i}^{\max}$, $K = 54$, and $N^{\min} = 63$, as a function of $\Delta_{t,i}$ from (2), and for several values of p^{RS}. We observe that g_{coding} is significant and fast increasing with $\Delta_{t,i}$ and p^{RS}. We note that for large $\Delta_{t,i}$ the PER of the adaptive coding scheme becomes extremely small, and g_{coding} converges to $1/(1 - p_{\text{packet}}^{\text{RS}}(N^{\min}))$ as observed in Figure 1.

2) Energy Consumption for Transmission: Since instead of $N^{\min}$ symbols, we opportunistically transmit $N_{t,i}^{\text{actual}}$ symbols per packet, the potential gain of the adaptive coding scheme over the fixed code in terms of PER is achieved at the cost of higher energy consumption for per-packet transmission. This may seem to be a challenge for UWAC networks, where often energy resources at (battery-operated) network nodes are limited. However, considering the low reliability in UWAN links, and accordingly the energy spent for successfully received data packets, the improved error correction capability of the adaptive coding scheme may ultimately reduce energy consumption for transmission, as we discuss next.

Let $p_{\text{packet}}(N)$ be the error rate of a packet transmitted using an (K, N) error-correction code. Then, a successful transmission requires on average

$$M(N) = \frac{1}{1 - p_{\text{packet}}(N)} \tag{6}$$

packet transmissions. Furthermore, denoting by P and T_{h} the transmit power and duration of the packet header and preample sequence, respectively, the average energy consumption for one successful packet transmission is $M(N) \cdot P(NT_s + T_{\text{h}})$. To quantify the advantage of our adaptive coding approach in terms of transmission-energy consumption we consider the ratio

$$g_{\text{energy}} = \frac{M(N^{\min}) \cdot (N^{\min} T_{\text{s}} + T_{\text{h}})}{M(N_{t,i}^{\text{actual}}) \cdot (N_{t,i}^{\text{actual}} T_{\text{s}} + T_{\text{h}})} \,. \tag{7}$$

We note that g_{energy} in (7) increases with T_{h}, and is influenced by $N_{t,i}^{\text{actual}}$ through the energy consumption term $PN_{t,i}^{\text{actual}} T_{\text{s}}$ and the average number of packet transmissions $M(N_{t,i}^{\text{actual}})$, where the latter depends through (6) on the packet error rate (PER) $p_{\text{packet}}(N_{t,i}^{\text{actual}})$. Hence, $M(N_{t,i}^{\text{actual}})$ decreases with $N_{t,i}^{\text{actual}}$, while the energy consumption term increases for larger $N_{t,i}^{\text{actual}}$.

To shed some light on the value of g_{energy} from (7), we consider the example of the RS code used already in Section III-A1. In Figure 2, we show g_{energy} from (7) as a function of $\Delta_{t,i}$ (2) and T_{h}, and the same set of parameters considered in Section III-A1. In particular, $N_{t,i}^{\text{actual}} = N_{t,i}^{\max}$. We note that while g_{energy} increases with T_{h}, due to the low transmission rate this increase is not significant. As expected, we observe that the curves have a distinct maximum, reflecting the trade-off between larger transmission energy and lower PER for increasing $N_{t,i}^{\max}$. We note that g_{energy} increases with larger symbol-error rate p^{RS}, as it emphasizes the error-rate gain of adaptive over fixed-rate coding. Furthermore, we observe that the ratio g_{energy} is larger than one in a wide range of distances $\Delta_{t,i}$ for $p^{\text{RS}} \geq 0.08$. Hence, adaptive coding consistently provides a gain in energy consumption in such unreliable communication channels, which are typical for UWANs.

Considering the convergence of g_{coding} from (5) to a constant gain value as shown in Figure 1, and the non-monotonic behavior of g_{energy} from (7) as can be seen from Figure 2, we note that the choice of $N_{t,i}^{\text{actual}} = N_{t,i}^{\max}$ can be improved upon, especially for large values of $\Delta_{t,i}$. In particular, to limit energy consumption, we optimize $N_{t,i}^{\text{actual}}$, as described in the following.

B. Optimization of $N_{t,i}^{\text{actual}}$

The channel between transmitter i and receiver j at time t is characterized by its capacity $C_{t,i,j}$, whose unit is bit per coded symbol. Assuming that channel conditions do not change much within a packet transmission, the receiver can likely successfully decode after $N_{t,i}^{\text{actual}}$ transmitted symbols if

$$C_{t,i,j} N_{t,i}^{\text{actual}} \geq (1 + \delta) KL \,, \tag{8}$$

where L is the byte size of coded symbols and δ accounts for the gap to capacity using practical codes. Hence, by estimating $C_{t,i,j}$ transmitter i can determine the number of symbols required for successful decoding. Combining (8) with adaptation based on interference range, for a single packet transmission we have

$$N_{t,i}^{\text{actual}} = \min\left(\frac{(1+\delta)KL}{C_{t,i,j}}, N_{t,i}^{\max}\right) . \tag{9}$$

We note that $N_{t,i}^{\text{actual}}$ according to (9) could be below $N^{\min}$, which would lead to energy savings compared to the fixed-rate coding scheme.

As an example of obtaining $N_{t,i}^{\text{actual}}$, we consider the M-ary symmetric channel (MSC) and the M-ary erasure channel (MEC). The former model is a good fit for the RS code discussed in Section III-A, and the latter is used for rateless Fountain codes, discussed further below. For the case of RS coding and the MSC, we have $M = 2^L$ symbols and the capacity is

$$C_{t,i,j} = L - H\left(p_{t,i,j}^{\text{RS}}\right) - p_{t,i,j}^{\text{RS}} \log_2(M-1) , \tag{10}$$

where $H(\cdot)$ is the binary entropy function. For the MEC model with symbol erasure probability $p_{t,i,j}^{\text{e}}$, we have

$$\boldsymbol{C}_{t,i,j} = L\left(1 - p_{t,i,j}^{\text{e}}\right) . \tag{11}$$

For (10) and (11), estimates $\hat{p}_{t,i,j}^{\text{RS}}$ and $\hat{p}_{t,i,j}^{\text{e}}$ of the symbol error and erasure rates, respectively, are required. The process of obtaining these estimates is described next for both single and multiple packet transmissions.

1) Single Packet Transmission: If a feedback channel exists (as assumed in [9]), the receiver can measure the channel conditions (e.g., from a received request-to-send packet) and report $C_{t,i,j}$ to the transmitter, which then directly calculates $N_{t,i}^{\text{actual}}$ from (9). Otherwise, since both $p_{t,i,j}^{\text{RS}}$ from (10) and $p_{t,i,j}^{\text{e}}$ from (11) can be represented as a function of the SNR, $\text{snr}_{t,i,j}$, we use the distance information available at the transmitter and an attenuation model to obtain an estimate for $\text{snr}_{t,i,j}$ and calculate $C_{t,i,j}$.

2) Multiple Packet Transmission: In a communication session between nodes i and j, multiple packets may be transmitted and acknowledgments are received for successful packets. By knowing the number of symbols needed for a previous successful transmission, and assuming channel conditions do not change much between consecutive packets, the transmitter can reverse (9) to estimate $C_{t,i,j}$. In the case of unsuccessful (and thus unacknowledged) previous packets, we gradually update the assumed channel conditions. For an unsuccessful packet $m-1$ transmitted at time t_{m-1}, if $N_{t_{m-1},i}^{\text{actual}} < N_{t_{m-1},i}^{\max}$ we have

$$\begin{aligned} p_{t_{m-1},i,j}^{\text{RS}} &> \hat{p}_{t_{m-1},i,j}^{\text{RS}} , \\ p_{t_{m-1},i,j}^{\text{e}} &> \hat{p}_{t_{m-1},i,j}^{\text{e}} . \end{aligned} \tag{12}$$

Thus, we monotonically increase $\hat{p}_{t,i,j}^{\text{RS}}$ or $\hat{p}_{t,i,j}^{\text{e}}$ till a threshold is reached or the number of retransmitted packets exceeds a maximum P, after which failure is declared and the packet is dropped. Given distance information between i and j, $d_{t_m,i}$, the above threshold can be calculated from an upper bound on the signal attenuation (e.g., [15]). Note that the above process does not involve direct estimate of link quality and does not require additional communication overhead other than acknowledgments, which are already part of any ARQ protocol.

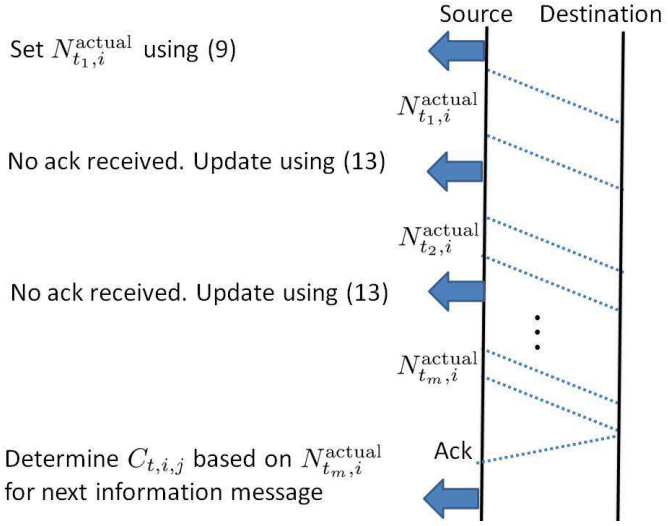

Fig. 3: Illustration of the procedure of updating channel conditions for multiple packet transmission.

We observe the similarities in the problem of increasing $\hat{p}_{t,i,j}^{\text{RS}}$ or $\hat{p}_{t,i,j}^{\text{e}}$, and the congestion avoidance mechanism of the TCP-IP protocol [16]. In TCP-IP, congestion avoidance is required to manage failures in packet transmission by changing the congestion window, such that for each unacknowledged packet the maximal window size is halved and the window size is reduced to its initial value. Adopting the same strategics, we set

$$\begin{aligned} \hat{p}_{t_m,i,j}^{\text{RS}} &= \hat{p}_{t_{m-1},i,j}^{\text{RS}} \cdot x_{\text{MSC}} , \\ \hat{p}_{t_m,i,j}^{\text{e}} &= \hat{p}_{t_{m-1},i,j}^{\text{e}} \cdot x_{\text{MEC}} , \end{aligned} \tag{13}$$

where $x_{\text{MSC}} > 1$ and $x_{\text{MEC}} > 1$ control the trade-off between energy consumption for transmission and the number of packets needed till successful decoding, i.e., network latency. An illustration of the above procedure is presented in Figure 3.

C. Extension to IR-HARQ

The process of optimizing $N_{t,i}^{\text{actual}}$ is extended next to use in the IR-HARQ protocol (cf. [4]). In the IR-HARQ protocol, instead of packet-wise decoding, the designated receiver accumulates all demodulated symbols from previous packets. In turn, the source keeps transmitting packets until an acknowledgement of successful decoding is received. In this section, we describe how our adaptive coding scheme can be embedded in such protocol.

Consider unsuccessful transmission of previous packets, $n = m', \ldots, m-1$. Assuming channel conditions do not

change much from packet m' to m, we modify (9) into

$$N_{t_m,i}^{\text{actual}} = \min\left(\frac{(1+\delta)KL - C_{t_m,i,j}\sum_{n=m'}^{m-1} N_{t_n,i}^{\text{actual}}}{C_{t_m,i,j}}, N_{t_m,i}^{\max}\right), \tag{14}$$

and $C_{t_m,i,j}$ is updated using the same process illustrated in Figure 3 for multiple packet transmission. Similar to the case of multiple packet transmission discussed in Section III-B2, the initial estimate $C_{t_{m'},i,j}$ required to calculate $N_{t_{m'},i}^{\text{actual}}$, is set by the number of symbols, $\sum_{n=m''}^{m'-1} N_{t_n,i}^{\text{actual}}$, needed for successful decoding of a previous message accomplished after $m'-m''$ packet transmissions.

IV. Implementation

We now describe practical implementation schemes for our adaptive coding approach. Let

$$N^{\max} = N^{\min} + \frac{d^{\max}}{T_{\text{s}} \cdot c}\,. \tag{15}$$

Since $N^{\min}$ and $N^{\max}$ are set by the maximal and minimal propagation delay of the system, respectively, by (3), $N^{\min} \le N_{t,i}^{\max} \le N^{\max}$. While node i has knowledge of $\Delta_{t,i}$ and thus can calculate $N_{t,i}^{\max}$ to set $N_{t,i}^{\text{actual}}$ according to (9) or (14), this may not be the case for its receiver j, who is aware of only $N^{\min}$, $N^{\max}$, and K. This is because node j may not be aware of the distance of node i to all nodes within its interference range. Considering this problem, one possibility for node i is to transmit the value $N_{t,i}^{\text{actual}}$ as a separate header packet. If it is undesirable to transmit this side information, which of course takes away from the available guard time for sending extra parity symbols, the iterative decoding scheme illustrated in Figure 4 can be applied for the case of a single packet transmission. In this case, the receiver makes multiple decoding attempts with the first attempt starting after receiving enough information bits to satisfy (8). If decoding fails (e.g., the cyclic-redundancy check (CRC) did not pass), receiver j makes another attempt after having obtained at least one more demodulated symbol. Hence, at most $M^{\text{try}} = N^{\max} - (1+\delta)K + 1$ decoding attempts are made. Unfortunately, this approach cannot be used in an IR-HARQ protocol. Here, since the order of demodulated symbols from multiple packets is important for decoding, successive decoding cannot be made and a post-amble signal is transmitted to mark the position of the last symbol in each packet.

Next, we suggest two implementation examples for our adaptive coding approach.

1) Bank-of-Codes: The first implementation uses a pre-defined bank of up to $N^{\max} - (1+\delta)K$ codes, which can be a set of either optimized codes for different rates or punctured codes. For the latter, we apply an (K, N) *mother code*, where N is pre-defined at both transmitter and receiver. Since $N_{t,i}^{\text{actual}} \le N_{t,i}^{\max}$, for a single packet transmission, $N \ge N^{\max}$, while for IR-HARQ, $N \ge P \cdot N^{\max}$ (recall P is the maximum allowed number of packet retransmissions). At its designated time slot t, node i transmits $N_{t,i}^{\text{actual}}$ symbols by puncturing $N - N_{t,i}^{\text{actual}}$ symbols of the codeword, following a pre-defined puncturing pattern, which, in the case of an IR-HARQ, is different for every packet transmission.

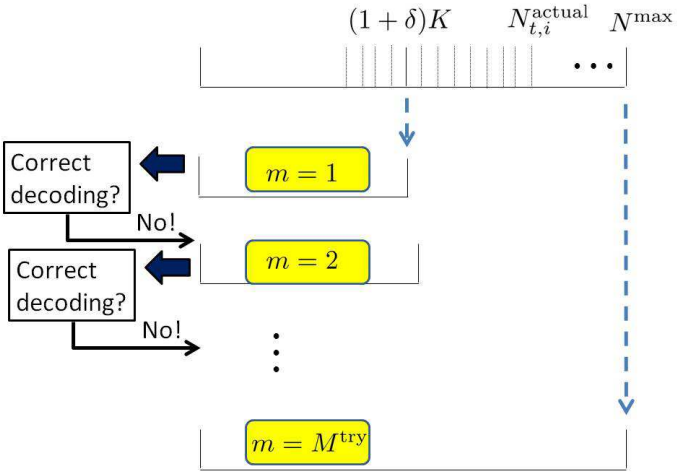

Fig. 4: Illustration of adaptive coding implementation for single packet transmission.

2) Rateless Codes: The second implementation example is based on Fountain codes [17]. At time t, the transmitter generates a codeword whose length corresponds to $N_{t,i}^{\text{actual}}$ symbols. Due to the rateless nature of Fountain codes, generation of any number of parity symbols is easily facilitated, and the process is similar in both single packet transmission and IR-HARQ. No side information is needed at the receiver assuming that a common seed for the random generation of the columns of the generator matrix is used. The same adaptive coding and successive decoding procedure can be applied to variants of Fountain codes, most notably Raptor codes [18]. For Raptor codes, we use an (K, N^{outer}) outer error-correction code and an inner $(N^{\text{outer}}, N_{t,i}^{\text{actual}})$ Fountain code, where $N^{\text{outer}} = \beta \cdot K$ and β is a design parameter controlling the maximal probability of the failure of the inner Fountain decoding.

With regards to Fountain codes, using LT Fountain codes [19] has a benefit if the transmitter-receiver link can be modeled as an erasure channel. In this case, message passing decoding is alike successive cancelation, and additionally demodulated symbols available at the m-th decoding attempt can be used directly to improve the result from the $(m-1)$-st decoding stage (see [17]). Here, decoding with and without knowledge of $N_{t,i}^{\text{actual}}$ are in fact identical, and thus there is no complexity overhead due to the iterative decoding procedure from Figure 4. However, since in underwater acoustic communication transmission rate is on the order of a few kbps and packets are small [20], we expect K to be on the order of a few hundreds to thousand symbols. Therefore, since popular LT and Raptor codes perform well only for large code word lengths, for our numerical results we apply the Fountain coding scheme described in [21], where good performance results are obtained for information word lengths as low as $K = 100$, at

the cost of somewhat increased decoding complexity. When the channel cannot be modeled as an erasure channel, the integration of newly arrived samples into message-passing decoding is somewhat more complicated. For this case, favorable decoding schedules are described in [22] and [23].

3) Discussion: Comparing the above Bank-of-Codes and Rateless coding schemes, we note that for the former, since often there are restrictions for the code design parameters[1], N may be much bigger than $N^{\max}$ (for a single packet transmission) or $P \cdot N^{\max}$ (for IR-HARQ), and encoding and decoding complexity may be greater than that of the rateless scheme. However, in the Bank-of-Codes scheme, the punctured or pre-defined code can specifically be optimized for a rate and thus achieve better performance than the rateless code.

V. Performance Results and Discussion

We now evaluate the performance of our adaptive coding scheme in terms of the PER, energy consumption for transmission, and throughput using numerical simulations. Furthermore, to show the effect of a realistic sea environment, we also present results from a sea trial, where we implemented the punctured RS scheme in an actual underwater acoustic modem (namely, the Deep-Link modem).

A. Simulations

1) Setting: Our simulation setting includes a Monte-Carlo set of 10000 channel realizations. For each channel realization, four nodes are uniformly randomly placed in a square area of 2000×2000 m^2 at a fixed depth of 40 m for a 50 m long water column. The nodes operate for 100 sec in a TDMA network. Since in this paper, we are more interested in showing the possible gain of using our adaptive coding scheme rather than the absolute decoding capability, for simplicity in our simulations we adopt a binary erasure channel (BEC) model (i.e., MEC with $M = 2$ with binary phase shift keying (BPSK) modulation. The symbol-erasure probability is determined based on the transmitter-receiver link distance, d. More specifically, for each d, we calculate the receiver-side SNR using the Bellhop ray-tracing simulator (cf. [24]) for a flat sand surface, carrier frequency of 15 kHz, a common power source level of 130 dB//μPa@1m, and a noise level of 50 dB//μPa/Hz. The channel erasure rate is then determined from the calculated SNR considering the BPSK modulation. The output of the Bellhop simulator in terms of the transmission loss as a function of range is given in Figure 5. From the figure we observe that for different ranges we may get the same transmission loss and thus channel erasure rate, which is due to the shadowing characteristics of the underwater acoustic channel [1]. An approximate model of this transmission loss is

$$\mathrm{TL} = \gamma \log_{10}(d) + \alpha d/1000 \,, \qquad (16)$$

where d is the transmission distance. To allow channel changes (which affects $C_{t,i,j}$ from (8)), during the network operation

[1]For example, for Reed-Solomon codes N must be equal to $2^n - 1$ for some integer n [14].

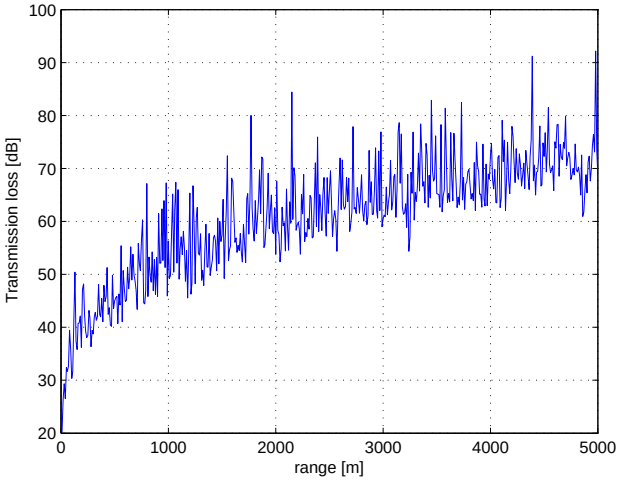

Fig. 5: Transmission loss vs. range. Output from the Bellhop simulator [24].

we let the nodes drift between the transmission of packets, and calculate the snr and the p^{e}, accordingly. Drift motion is simulated using the Shallow Water Hydrodynamic Finite Element Model (SHYFEM) ocean current model [25]. The model is set for location $49^o16'13.33''N,\ 126^o16'6.4''W$ (i.e., near Vancouver, BC), and a channel structure with two underwater hills at depth 30 m located at both corners of the considered square area.

During the network operation, out of the four nodes, we choose a transmitter and receiver, and set $N_{t,i}^{\mathrm{actual}}$ according to the maximal distance of the transmitter from its intended receiver and the nodes scheduled to transmit in time slots t and $t+1$. The transmitter sends short information messages of $K = 456$ bits with a transmission rate of 500 bps, $T_{\mathrm{h}} = 0.1$ sec, and an original code rate of $K/N^{\min} \approx 0.9$. The duration of the time slot is determined according to a maximal detection range of 1500 m and a propagation speed of 1500 m/sec. Hence, using the adaptive coding scheme, at most, i.e., for $d_{t,i} = 0$ m, 1000 coded symbols can be added to form a coding rate of $K/N^{\max} \approx 0.45$. Packets are retransmitted until successful reception is obtained at the intended receiver. This scenario mimics the exchange of navigation packets in the Deep-Link system [3]. We evaluate performance of IR-HARQ using the adaptive coding scheme with fully utilized time-slot *(FIR-HARQ)*, and IR-HARQ using optimized number of symbols *(OIR-HARQ)* To show the effect of using the IR-HARQ we also show results for a single packet transmission with a fixed coding gain *(Single)*. For the considered schemes, the maximal number of packet retransmissions allowed until a message is declared failed is $P = 5$. For the OIR-HARQ, the threshold for the updating of $\hat{p}^{\mathrm{e}}_{t,i,j}$ (see Section III-B2) is calculated from model (16) for $\gamma = 30$ and $\alpha = 3$ as an upper bound for power attenuation in the channel. Similarly, we use $\gamma = 10$ and $\alpha = 1.5$ as a lower bound on power attenuation to calculate the initial condition $\hat{p}^{\mathrm{e}}_{t_1,i,j}$ at the beginning of the network operation, and $\delta = 0.1$ for the ratio of required information bits in (8). As a worst

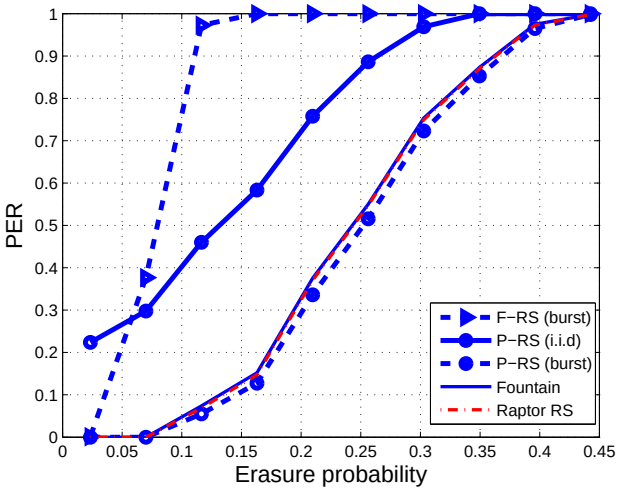

Fig. 6: PER as a function of channel erasure rate.

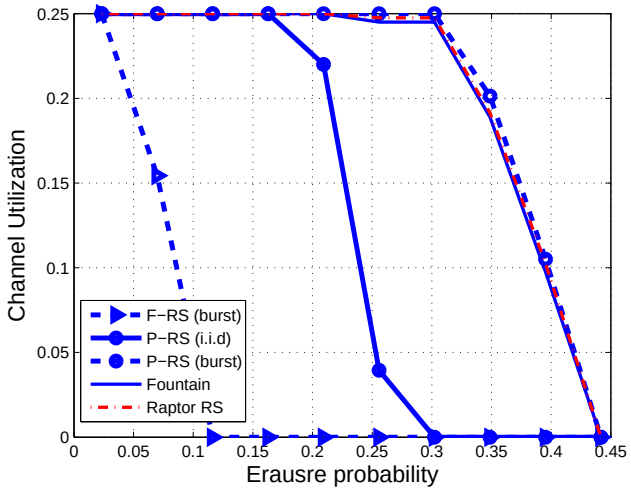

Fig. 7: Channel utilization as a function of channel erasure probability (for $\Delta_{t,i} \approx 650$ m).

case scenario for the comparison with the fixed-rate code, we assume acknowledgments are always received.

For the case of a single packet transmission (denoted above as Single), we demonstrate the gain of the adaptive coding scheme by showing performance of different coding implementations: RS (fixed *(F-RS)* and punctured *(P-RS)*), Fountain [21], and Raptor codes using an RS outer code (we note that similar values were obtained for Raptor codes using a low-density parity check (LDPC) outer code). As performance of the RS scheme varies greatly with the erasure patterns, we show performance results for both i.i.d. and burst-wise erasures. The former is motivated by the ambient noise in the channel, and the latter by temporarily correlated waves and ships-induced noises [1]. Finally, for the Raptor codes we use $\beta = 1.2$ (see Section III). A software implementation of these protocols can be downloaded from [26].

2) Results: We start off by comparing performance of the adaptive coding scheme to the fixed coding scheme for a single packet transmission, where for the former we transmit $N_{t,i}^{\max}$ symbols and for the latter we transmit $N^{\min}$ symbols. In Figure 6, we show the PER as a function of the erasure probability of the channel. For each value of erasure probability, we average the PER for the cases where the actual erasure probability is within a range of 0.02 from the one indicated through a marker in Figure 6. First, we observe that the performance of the RS scheme for burst-wise erasures is significantly better than that for i.i.d. erasures. This is due to the binary (BPSK) transmission and emphasizes on the suitability of RS coding in burst-noise channels. However, from Figure 6 we also see that even for i.i.d. erasures, the different adaptive coding schemes significantly outperform that with the fixed-rate RS code. The implementation with Fountain and Raptor codes shows its advantage for memoryless channels (i.i.d. erasures), and again greatly outperforms the fixed-rate coding scheme.

Next, we investigate channel utilization, defined as the rate of successful packets, for the different adaptive schemes. Since performance changes with both channel erasure probability and $\Delta_{t,i}$ from (2), in Figures 7 and 8 we show channel utilization as a function of the channel erasure provability and $\Delta_{t,i}$, respectively. The former figure is obtained by calculating channel utilization for cases where $\Delta_{t,i}$ is within the range of 640 ± 64 m, and the latter for cases where the channel erasure probability is within the range of 0.21 ± 0.02. Note that since we consider four nodes and TDMA, channel utilization is bounded from above by $\frac{1}{4}$. However, it can considerably degrade if retransmissions are needed. For example, as also shown by the results in Figure 6, for the considered erasure rate in Figure 8, only a few packets were properly decoded using the fixed RS code and channel utilization is almost zero. From both figures, we observe a significant gain of the adaptive coding schemes over the fixed-rate RS scheme. From Figure 8, it can be seen that, as expected, performance improves as $\Delta_{t,i}$ increases. As in Figure 6, the best performance is achieved by the punctured RS scheme for burst-wise erasures with only a very small performance loss for the Fountain and Raptor coding schemes. In fact, from Figures 7 and 8 we observe that for these schemes starting from $\Delta_{t,i} \approx 150$ m and channel erasure rate of up to 0.3, channel utilization is maximal, i.e., no retransmissions are required.

We now compare performance of the considered three protocols, namely: Single, FIR-HARQ, and OIR-HARQ. Due to the small difference between performance of the adaptive coding schemes, in the following we present results of only the binary Fountain code implementation. In Figure 9, we show the error $\rho_p(m) = |p^{\mathrm{e}} - \hat{p}^{\mathrm{e}}|$ as a function of packet number m for different values of x_{BEC}. Since motion in our simulations is restricted to drifting, p^{e} does not change rapidly, and $\rho_p(m)$ reflects convergence of estimate $\hat{p}^{\mathrm{e}}$. Since we bound the increase of $\hat{p}^{\mathrm{e}}$, $\rho_p(m)$ decreases fast after three packet transmissions. We also observe that the initial error (i.e., $\rho_p(1)$) increases with x_{BEC}. This is because the number of transmitted symbols till decoding increases with x_{BEC}, and the former is used to determine the initial $\hat{p}^{\mathrm{e}}$. Clearly, ρ_p decreases for smaller x_{BEC} values. This means less transmitted symbols per packet, but at the cost of transmitting more

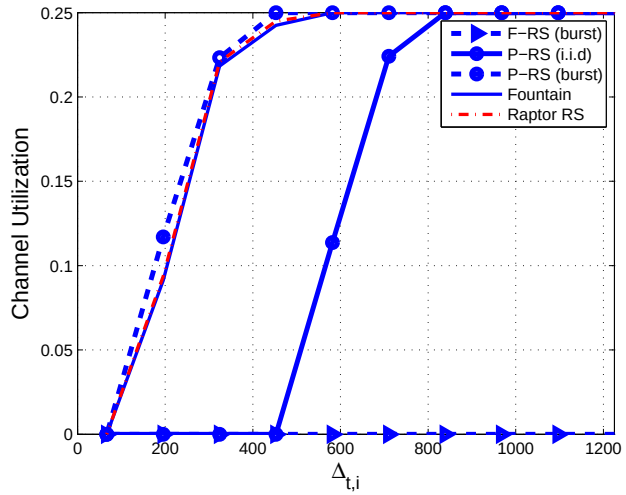

Fig. 8: Channel utilization as a function of $\Delta_{t,i}$ (for erasure probability of roughly 0.21).

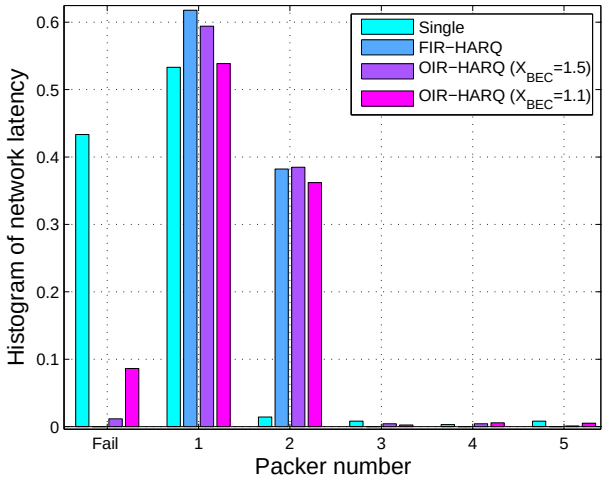

Fig. 10: Histogram of network latency in terms of number of packets needed till decoding.

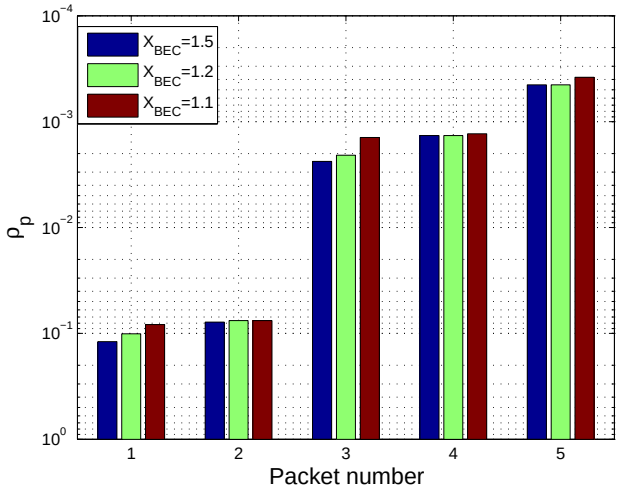

Fig. 9: Error $\rho_p(m)$ as a function of packet number m. (Note that values in the y-axis are reversed).

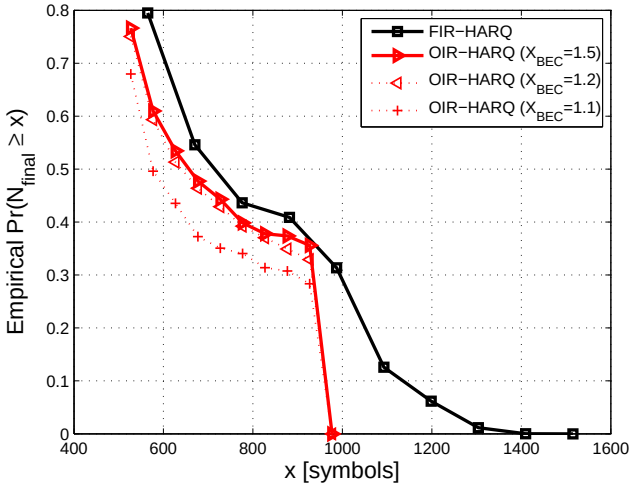

Fig. 11: CDF of the number of symbols transmitted till successful decoding, N_{final}.

packets. However, as observed in Figure 9, the difference is not significant. To determine the effect of x_{BEC} on network latency, in Figure 10 we show a histogram of the number of packets needed till decoding is possible. We observe that failure rate of the Single scheme is far greater than that of the IR-HARQ schemes. In fact, no failures are detected for the FIR-HARQ scheme, which utilizes the entire time slot. As expected, latency decreases for higher values of x_{BEC}. However, the latter characteristic comes at the cost of energy consumption for transmission, which improves as the number of transmitted symbols needed for successful decoding, $N_{\text{final}} = \sum_{m=1}^{P} N_m$, decreases. This is observed in Figure 11, where we show the cumulative density function (CDF) of N_{final}. We note the large variance of N_{final} for the FIR-HARQ method, for which the number of redundancy symbols greatly increases as more packets are required for decoding. Due to the adaptive transmission in the OIR-HARQ schemes, their N_{final}, and thus energy consumption for transmission, is significantly lower than the FIR-HARQ scheme. Here, we observe that N_{final} does not change much for $x_{\text{BEC}} = 1.5$ and 1.2, which implies that our adaptive coding scheme is not very sensitive to the choice of this parameter.

Finally, in Figure 12 we show the CDF of the network goodput, defined as the number of delivered information bits during the network operation of 100 sec. As expected, goodput of the IR-HARQ schemes is considerably higher than that of the Single scheme. We also note that goodput is maximal for the FIR-HARQ scheme (at the cost of energy-consumption for transmission). However, not much difference is observed comparing performance of FIR-HARQ and OIR-HARQ with $x_{\text{BEC}} = 1.5$. By these results, we argue that utilizing the time slot to adaptively adjust the code rate decreases network latency and increases network goodput. Furthermore, optimizing

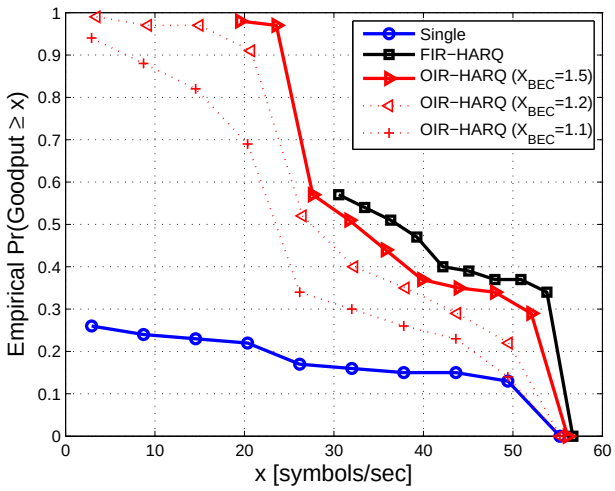

Fig. 12: CDF of network goodput.

the coding rate in an IR-HARQ scheme significantly reduces energy consumption for transmission at a small cost in network goodput.

B. Sea Trial Results

To measure the performance of our adaptive scheme in a realistic sea environment, in November 2009 we conducted an experiment in the Haifa harbor, Israel. The experiment included three Deep-Link modems, statically deployed from the harbor docks as shown in Figure 13. The distance was 340 m between nodes 1 and 2 *(Link 1)*, 780 m between nodes 1 and 3 *(Link 2)*, and 910 m between nodes 2 and 3 *(Link 3)*. The modems used RS codes with flexible parameters. Erasure decoding was performed, where erasures were declared based on thresholding the received signal samples. Using this capability, we tested both the fixed and punctured RS coding schemes. During the experiment, the three nodes periodically broadcasted short packets of 200 bits at a rate of 300 bps in a TDMA scheduling scheme, where in each time frame first node 1 transmits, then node 2, and then node 3. Each packet included a header of 0.67 sec for a synchronization signal and preamble sequence, and each time slot included a guard interval accounting for possible clock drifts and a maximal propagation delay of 1 sec. The latter was determined according to the size of the harbor, which was roughly 1500 m. We compared the performance of a single packet transmission using the punctured RS scheme with a fixed RS code of rate $4/5$, such that the duration of the time slot was roughly 2.5 sec, and at most, i.e., for $d_{t,i} = 340$ m, coding rate of the punctured RS scheme was 0.41.

The experiment included two parts each lasting for one hour. In the first part we measured performance of the fixed RS coding scheme, and in the second part the punctured RS coding scheme was tested. Signals were transmitted at a low source level of 130 dB//μPa@1m.

In Figure 14, we show the packet success rate, P_{success}, for the three links. Similar to the simulated results in Figure 6, we observe a significant gain of the adaptive over the fixed

Fig. 13: Satellite picture of the experiment location (picture taken from Google Earth on July 23, 2012.) The three locations of the nodes are marked.

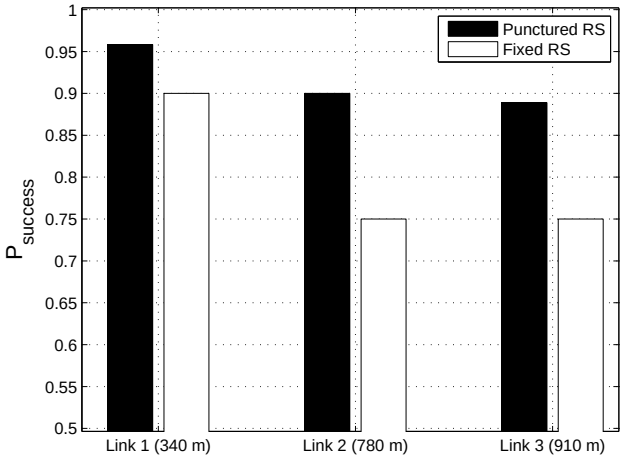

Fig. 14: Packet success rate for the three links from the sea trial.

coding scheme, which is 14% on average. The success rate increases also for Link 1, where transmission distance is short and thus the PER has been low even for fixed-rate coding. We can thus conclude that the proposed adaptive coding scheme is indeed a viable approach to increase network goodput and decrease energy consumption in a realistic UWAN.

VI. Conclusions

In this paper, we suggested an adaptive coding approach to improve the packet error rate in a time-slotted UWAC network. Different from usual adaptive coding approaches, our approach uses range information as the basis for adaptation of the code rate. This allows us to exploit the difference between the worst-case and the actually required guard time. By optimizing the number of parity check symbols transmitted in both single packet transmission and multiple packet transmission using IR-HARQ, we managed to control the trade-off between goodput and energy consumption for transmission. We described two implementations for our approach, using punctured and rateless codes. By means of analysis and simulation results, we demonstrated the advantages of our adaptive coding scheme over fixed-rate error correction in terms of packet error rate,

transmission energy consumption, and throughput. The simulation results were verified in a sea trial.

REFERENCES

[1] W. Burdic, *Underwater Acoustic System Analysis*. Los Altos, CA, USA: Peninsula Publishing, 2002.

[2] M. Chitre, S. Shahabudeen, L. Freitag, and M. Stojanovic, "Recent advances in underwater acoustic communications and networking," in *IEEE Oceans Conference*, sep. 2008, pp. 1–10.

[3] *Specifications of the Deep-Link system*. Rafael Ltd., http://www.rafael.co.il/marketing/SIP_STORAGE/FILES/5/995.pdf.

[4] C. Lott, O. Milenkovic, and E. Soljanin, "Hybrid ARQ: Theory, state of the art and future directions," in *IEEE Information Theory Workshop on Information Theory for Wireless Networks*, Jul. 2007, pp. 1–5.

[5] B. Tomasi, L. R. Laura Toni, Paolo Casari, and M. Zorzi, "Performance study of variable-rate modulation for underwater communications based on experimental data," in *IEEE OCEANS*, Seattle, USA, Sep. 2010.

[6] M. Chitre and M. Motani, "On the use of rate-less codes in underwater acoustic file transfers," in *IEEE OCEANS*, Jun. 2007.

[7] P. Casari, M. Rossi, and M. Zorzi, "Towards optimal broadcasting policies for HARQ based on fountain codes in underwater networks," in *IEEE/IFIP WONS*, Jun. 2008.

[8] Z. Haojie, H. Tan, A. Valera, and B. Zijian, "Opportunistic ARQ with bidirectional overhearing for reliable multihop underwater networking," in *IEEE OCEANS*, Sydney, Australia, May 2010.

[9] B. Tomasi, D. Munaretto, J. Preisig, and M. Zorzi, "Real-time redundancy allocation for time-varying underwater acoustic channels," in *ACM international conference on Underwater Networks and Systems (WUWNet)*, Los Angeles, USA, Nov. 2012.

[10] X. Guo, M. Frater, and M. Ryan, "Design of a propagation-delay-tolerant MAC protocol for underwater acoustic sensor networks," *IEEE J. Oceanic Eng.*, vol. 34, no. 2, pp. 170–180, Apr. 2009.

[11] H. H. Ng, W. S. Soh, and M. Motani, "ROPA: A MAC protocol for underwater acoustic networks with reverse opportunistic packet appending," in *IEEE Wireless Communications and Networking Conference (WCNC)*, Sydney, Australia, Apr. 2010.

[12] M. Erol, H. Mouftah, and S. Oktug, "Localization techniques for underwater acoustic sensor networks," *IEEE Commun. Mag.*, vol. 48, no. 12, pp. 152–158, Jun. 2010.

[13] R. Diamant and L. Lampe, "Underwater localization with time-synchronization and propagation speed uncertainties," *IEEE Trans. Mobile Comput.*, vol. PP, no. 99, p. 1, 2012.

[14] S. Wicker and V. Bhargava, *Reed-Solomon Codes and Their Applications, Chap. 7*. New York, USA: IEEE Press, 1994.

[15] R. Diamant, H. Tan, and L. Lampe, "LOS and NLOS classification for underwater acoustic localization," *Accepted for the IEEE Transactions on mobile Computing*, Nov. 2012, available online on http://ece.ubc.ca/∼roeed/$\mathrm{index}_{\mathrm{files}}$/publications.htm.

[16] D. Comer, *Internetworking with TCPIP:Principles, Protocols, and Architecture*, 5th ed. Prentice Hall, 2006.

[17] D. MacKay, "Fountain codes," *IEE Proceedings-Communications*, vol. 152, no. 6, pp. 1062–1068, Dec. 2005.

[18] A. Shokrollahi, "Raptor codes," *IEEE Transactions on Information Theory*, vol. 52, no. 6, pp. 2551–2567, Jun. 2006.

[19] M. Luby, "LT codes," in *The IEEE Symposium on Foundations of Computer Science*, 2002, pp. 271–280.

[20] P. Casari and M. Zorzi, "Protocol design issues in underwater acoustic networks," *Elsevier Computer Communications*, vol. 34, no. 17, pp. 2013–2025, Jun. 2011.

[21] C. Studholme and I. F. Blake, "Random matrices and codes for the erasure channel," *Algorithmica*, vol. 56, no. 4, pp. 605–620, 2010.

[22] K. Hu, J. Castura, and Y. Mao, "Reduced-complexity decoding of Raptor codes over fading cannels," in *IEEE Global Commun. Conf. (GLOBCOM)*, San Francisco, CA, USA, Nov. 2006.

[23] A. AbdulHussein, A. Oka, and L. Lampe, "Decoding with early termination for Raptor codes," *IEEE Communications Letters*, vol. 12, no. 6, pp. 444–446, Jun. 2008.

[24] M. Porter and H. Bucker, "Gaussian beam tracing for computing ocean acoustic fields," *Journal of Acoustical Society of America*, vol. 82, no. 4, pp. 1349–1359, Oct. 1987.

[25] G. Umgiesser, "Shyfem finite element model for coastal seas, user manual," Apr. 2012, https://sites.google.com/site/shyfem/file-cabinet, Apr. 2012. [Accessed: Apr. 2012].

[26] R. Diamant, *MATLAB implementation for the adaptive coding protocols*, http://www.ece.ubc.ca/∼roeed.